Biochemical Society Transactions (2022) **50** 95–105
https://doi.org/10.1042/BST20210433

Review Article

Three-dimensional insights into human enveloped viruses *in vitro* and *in situ*

Naveen Vankadari[1], Doulin C. Shepherd[2], Stephen D. Carter[3] and Debnath Ghosal[2]

[1]Monash Biomedicine Discovery Institute and Department of Biochemistry and Molecular Biology, Monash University, Melbourne, VIC, Australia; [2]Department of Biochemistry and Pharmacology, Bio21 Molecular Science and Biotechnology Institute, The University of Melbourne, Melbourne, VIC, Australia; [3]Centre for Virus Research, Medical Research Council-University of Glasgow Centre for Virus Research, Glasgow, U.K.

Correspondence: Debnath Ghosal (debnath.ghosal@unimelb.edu.au) or Stephen D. Carter (stephen.carter@glasgow.ac.uk)

Viruses can be enveloped or non-enveloped, and require a host cell to replicate and package their genomes into new virions to infect new cells. To accomplish this task, viruses hijack the host-cell machinery to facilitate their replication by subverting and manipulating normal host cell function. Enveloped viruses can have severe consequences for human health, causing various diseases such as acquired immunodeficiency syndrome (AIDS), seasonal influenza, COVID-19, and Ebola virus disease. The complex arrangement and pleomorphic architecture of many enveloped viruses pose a challenge for the more widely used structural biology techniques, such as X-ray crystallography. Cryo-electron tomography (cryo-ET), however, is a particularly well-suited tool for overcoming the limitations associated with visualizing the irregular shapes and morphology enveloped viruses possess at macromolecular resolution. The purpose of this review is to explore the latest structural insights that cryo-ET has revealed about enveloped viruses, with particular attention given to their architectures, mechanisms of entry, replication, assembly, maturation and egress during infection. Cryo-ET is unique in its ability to visualize cellular landscapes at 3–5 nanometer resolution. Therefore, it is the most suited technique to study asymmetric elements and structural rearrangements of enveloped viruses during infection in their native cellular context.

Introduction

Enveloped viruses constitute a large structurally heterogeneous group of viruses and many have irregular and asymmetric elements associated with their virions. For example, the absence of helical symmetry in matrix protein layers (influenza A virus (IAV), respiratory syncytial virus (RSV) and Ebola virus), lack of global symmetry in capsid cores (HIV-1), and flexibility of glycoproteins (SARS-CoV-2) pose a challenge to structural biology. For example, isolated HIV-1 capsid cores are heterogenous and recalcitrant to crystallization. Likewise, looking at these structures by cryo-EM single particle analysis (SPA) would involve breaking up their individual components into homogenous particles. Cryo-electron tomography (cryo-ET) is uniquely suited for this as it allows investigation of the pleomorphic structural details of enveloped viral particles *in vitro* and within their native environment, 'the cell'. There are hundreds of pleomorphic enveloped viruses responsible for a wide range of human diseases. Until recently, structural details of their entry, replication, assembly, maturation and egress remained poorly understood. Cryo-ET's ability to unravel high-resolution structures of these viruses in an 'artifact-free' frozen-hydrated state is not only revolutionizing our understanding of enveloped virus structure but now has the potential to help in the development of novel therapeutics and vaccines against these clinically important viruses.

Envelope viruses are genetically diverse, exhibit a wide range of morphologies, and employ diverse entry steps, genome replication strategies and assembly mechanisms. Many enveloped viruses acquire their lipid envelopes from the host plasma membrane through a process known as budding. Other

Received: 14 September 2021
Revised: 22 December 2021
Accepted: 23 December 2021

Version of Record published: 25 January 2022

Biochemical Society Transactions (2022) **50** 95–105
https://doi.org/10.1042/BST20210433

enveloped viruses exist that acquire their membranes via the secretory pathway (poxviruses and flaviviruses), and sometimes this occurs before additional budding and fusion transformations with other membranous organelles, such as the nuclear envelope (herpes simplex viruses) [1,2]. During budding, the virally encoded envelope proteins are captured along with host-derived membrane proteins. The viral envelope proteins can either function in attachment or fusion with the host membrane and are usually glycosylated to assist with crucial roles in infectivity, protein folding, tropism, proteolytic processing and escape immuno-surveillance [3,4]. Before entering the host, the viral envelope serves to compartmentalize the viral genetic material (DNA or RNA) with structural and accessory proteins. Fusion between the virus envelope and host membrane allows release of the viral DNA or RNA into the host cell to sites of replication via endocytic or non-endocytic pathways [5]. Following fusion, some enveloped viruses use specialized packaging systems to deliver their viral genomes into the nucleus where genome replication and transcription occur (HIV-1 and IAV). Others, use similar strategies to release their genomes into the cytoplasm where viral replication factories are formed via the alteration of host cell pathways such as the secretory or autophagy pathways [6]. With the advent of cryo-ET, we are beginning to understand the structural details of many of these processes at unprecedented resolution.

In cryo-ET, plunge-frozen samples are imaged using a transmission electron microscope. A series of two-dimensional (2D) projection images are recorded as the frozen sample is rotated around an axis to first generate a 'tilt-series'. A three-dimensional (3D) volume of the object known as the 'tomogram' is calculated from these series of images, with resolution (3–5 nm) sufficient to make out the shapes and arrangements of large macromolecules [7]. To obtain higher-resolution structural information, repeating features within the tomogram can be computationally extracted (sub-tomograms), aligned, and averaged, a process known as 'subtomogram averaging' (STA), typically improving the resolution to ∼2–3 nm. For exceptionally favourable samples, however, STA is now capable of reaching ∼4 Å resolution, sufficient to build atomic models *de novo* [8].

Developments in microscope hardware (e.g. high-speed direct electron detection cameras, phase plates and high-precision stages) and data processing strategies are revolutionizing our ability to study macromolecular structures *in situ* using cryo-ET [8–15]. Moreover, interior parts of thick eukaryotic cells are now accessible by cryogenic Focused Ion Beam (cryo-FIB) milling. The most modern instruments are equipped with correlative light and electron microscopy (CLEM) workflows, greatly easing these processes [16,17]. Cryogenic correlated light and electron microscopy (cryo-CLEM) is an extension of the cryo-ET toolbox. In cryo-CLEM, proteins of interest are tagged with fluorescent labels and imaged by cryo-fluorescence to target specific and rare events using cryo-ET. As a result, we are now poised to 'see' how the machinery of enveloped viruses assembles and functions during various stages of the replication cycle and how the cell changes in response to infection.

The purpose of this review is to highlight important and exciting contributions of cryo-ET to structural virology, in particular for enveloped viruses. The first section will concentrate on recent cryo-ET imaging of human envelope virions from purified samples, whereas the second section will discuss how cryo-ET is revealing the molecular details of the viral life-cycle inside the host. There are tons of examples of cryo-ET studies of clinically relevant human enveloped viruses. However, owing to space constraints, we will discuss only six examples (HIV-1, SARS-CoV-2, HSV-1, Ebola virus, RSV and IAV) with a special emphasis on HIV-1, SARS-CoV-2, two of the most threatening viruses of present times.

Cryo-ET of reconstituted or purified enveloped viruses

HIV-1

HIV-1 belongs to the lentivirus genus of retroviruses and causes acquired immunodeficiency syndrome (AIDS). AIDS is caused by the gradual decline of infected immune cells, such as CD4+ T cells, macrophages and dendritic cells [18,19]. In recent years, AIDS-related mortality has declined through antiretroviral therapy (ART); however, at present, more than 9.5 million people of the 38 million people infected are without access to this treatment, especially in developing countries [20].

The mature infectious HIV-1 virion contains two copies of the viral RNA genome enclosed in the mature capsid core made of capsid protein (CA). Shortly after membrane fusion, entry of the capsid core is followed by reverse transcription of the viral RNA to double-stranded DNA (dsDNA) [21–23]. The dsDNA is associated with viral proteins, such as CA in a preintegration complex (PIC) [24–29], and enters the nucleus where the dsDNA ultimately integrates into the host cell chromosome [30]. The 55 kDa Gag polyprotein precursor is essential for virion assembly by the generation of membrane curvature through Gag oligomerization with

assistance from the cellular I-BAR protein IRSp53 at the inner leaflet of the plasma membrane [31,32]. Once budding is complete, the envelope containing the immature Gag shell undergoes scission from the cell via the ESCRT-III machinery [33]. The immature Gag shell is then cleaved by the virally encoded protease to produce several polypeptides — MA (matrix), NC (nucleocapsid), and CA (capsid). Cryo-ET imaging of purified HIV-1 virions has radically enhanced our understanding of the architecture of the capsid core, and its maturation process. As shown in Figure 1A, the first molecular model of an entire HIV-1 capsid core was derived using integrative approaches including cryo-ET of isolated cores at ~3 nm resolution, all-atom molecular dynamics (MD) simulations and cryo-EM SPA of tubular CA assembly [34]. The model shows a perfect fullerene cone made up of a lattice of CA protein (186 hexamers coloured in grey). Curvature leading to the assembly of a closed structure is accomplished by insertion of 12 pentamers (coloured in blue); seven pentamers towards the broad end and five pentamers toward the narrow end.

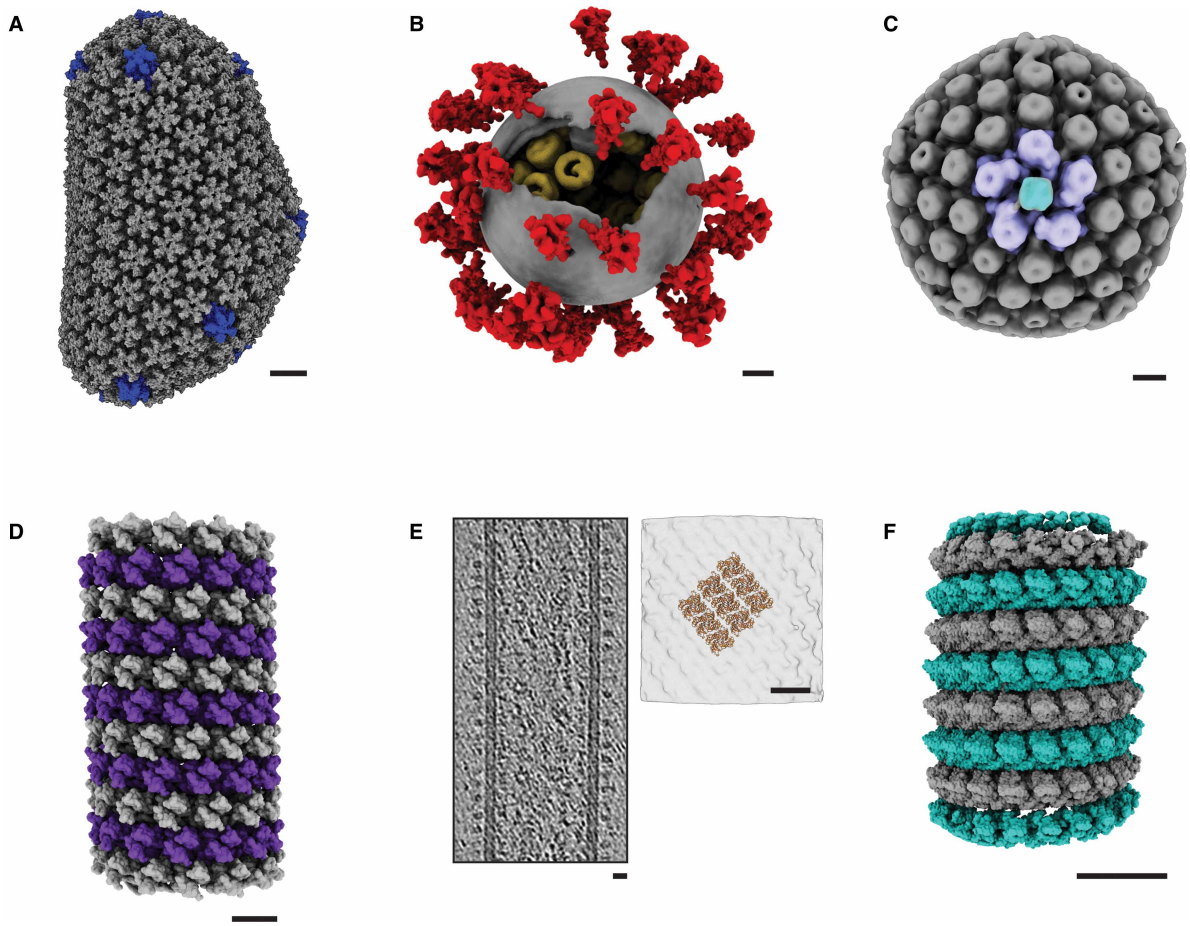

Figure 1. Structures of purified/reconstituted viruses determined by cryo-ET, STA and integrative methods.
(**A**) Structure of a mature HIV-1 capsid (PDB: 3J3Y); CA hexamers (grey), and pentamers (blue). (**B**) Ultrastructure of the SARS-CoV-2 (EMD-30430); lipid envelope (grey), S protein (red) and RNPs (gold). (**C**) Structure of a mature HSV-1 (EMD-5452). The portal structure is shown in cyan and the surrounding hexagons are coloured in purple. (**D**) Model of the Ebola virus nucleocapsid obtained by applying helical symmetry to NP subunits (grey and purple) from recombinant virus-like particles (PDB: 6EHM and EMD-3871). (**E**) Central slice through a tomogram of a respiratory syncytial virus (RSV) filament (left). Crystal structure of the RSV matrix protein (PDB: 4V23) docked into a subtomogram average of the RSV matrix protein [71]; matrix protein (gold), subtomogram average (translucent grey) (right). (**F**) Composite structure showing the IAV M1 matrix protein (translucent grey and turquoise) (EMD-22384) forms the matrix layer over the RNP (not visible). Scale bar 10 nm. Figures were made using publicly available atomic coordinates and maps from the protein data bank (PDB) and Electron Microscopy Data Bank (EMDB) using UCSF ChimeraX (Pettersen et al. 2021).

Biochemical Society Transactions (2022) **50** 95–105
https://doi.org/10.1042/BST20210433

In a more recent landmark study, Mattei et al. [35] showed the full structural power of cryo-ET and STA by revealing the precise molecular architecture of the natively assembled mature HIV-1 capsid core at 7 Å resolution. Some of the technicalities necessary for achieving the reported resolution included a dose-symmetric tilt acquisition scheme that optimally preserves high-resolution information, 3D CTF (contrast transfer function) correction and dose-filtering [36,37]. The precise positioning of each N-terminal domain (NTD) and C-terminal domain (CTD) within all CA hexamers showed that minor variations of tilt and twist observed between NTD and CTD are distributed over multiple CA–CA interfaces, likely allowing for variable curvature throughout the entire CA core. In addition, structures of the immature HIV-1 capsid using very similar STA approaches have provided fascinating insights into how the arrangement of the capsid proteins in the immature Gag lattice is vital for the regulation of cleavage into the mature infectious capsid by the viral protease [31,38–42].

SARS-CoV-2

SARS-CoV-2 is positive-sense single-stranded RNA (ssRNA) virus and belongs to the *Coronavirus* family. SARS-CoV-2 primarily infects the respiratory tract causing coronavirus disease (COVID-19) associated with severe acute respiratory distress syndrome (ARDS) [43]. To enter the cell, SARS-CoV-2 uses the virally encoded structural trimeric spike (S) protein to engage with human ACE2 [44–46]. Extensive structural analysis of the S protein has occurred during the COVID-19 pandemic [47–49]. Coronavirus genome replication takes place inside ER-derived double-membrane compartments [6,50]. The rapid application of cryo-ET during this time has resolved not only important architectural details about purified SARS-CoV-2 virions but also the ultrastructure of replication and assembly complexes in a frozen-hydrated state inside the host cell (see *in situ* section below).

At least four cryo-ET studies have demonstrated that purified inactivated clinical strains of SARS-CoV-2 are pleomorphic and contain ∼20–40 randomly distributed S trimeric proteins [51–54]. Many envelope viruses have genomes that are encapsulated with viral NC protein via extensive protein–protein interactions forming ribonucleoprotein (RNP) complexes. Using STA, Yao et al. revealed a reverse G-shaped model for the SARS-CoV-2 RNP complex from 2D class averages inside isolated virions (Figure 1B), which was comparable to a SARS-CoV-2 cryo-ET/STA RNP structures derived *in situ* [54,55]. Further 3D refinement provided insights into the 3D ultrastructure of the RNPs within the virions, including "eggs-in-a-nest" and 'pyramid'-shaped RNP architecture.

Ke et al. [44] used STA workflows to classify open and closed conformations of the S protein to reveal three states of the receptor-binding domain. Yao et al. [54] and Turoňová et al. [53] also observed similar receptor binding domain (RBD) conformational switching between prefusion S spikes. These works elegantly demonstrated how open and closed RBDs states observed in SPA cryo-EM studies of recombinant S trimers also take place on the virus surface, and most likely prime the receptor-binding sites for association with ACE2, as well as modulating antibody binding. Ke et al. Turoňová et al. and Yao et al. also used STA to resolve the positions of glycans on the surface of S and the presence of three hinges that allow it to flex up to 90° relative to the viral membrane. These findings are important because they show the various conformations these proteins adopt during purification could potentially alter their sensitivity to immune responses and how effective they are as vaccine immunogens [56]. In short, these studies provide evidence for how cryo-ET can efficiently examine the structure of new emerging viruses and provide robust tools to assess vaccine candidates during their development.

Cryo-ET of other enveloped viruses (HSV-1, Ebola virus, RSV, and IAV)

Here we highlight how cryo-ET has advanced our understanding of a few other pleomorphic and clinically important enveloped viruses.

Herpes simplex virus 1 (HSV-1) is a dsDNA virus in the alphaherpesvirus subfamily. HSV-1 exhibits both structured and pleomorphic elements. The dsDNA genome exhibits liquid-crystalline order when packaged into the icosahedral (T = 16) capsid shell [57]. A specialized structure, known as the portal, promotes the entry and packaging of the dsDNA viral genome during assembly [58–61] (Figure 1C). Cryo-ET has revealed the pleomorphic elements of HSV-1 virions, including polarization of the NC within virions, and a tegument (a specialized structure that occupies the space between the NC and the envelope) cap-like structure that contains 40 nm long-filaments (∼7 nm wide) close to the membrane [62]. Cryo-ET applied to primary enveloped

HSV-1 virions has also shown unique differences in virion size and shape compared with mature viruses [63]. Recently, cryo-ET/STA was used to classify the HSV-1 glycoprotein B natively arranged on virions in both pre-fusion and post-fusion conformations. However, resolution was limited to decern finer structural details [64]. In a recent study, Vollmer et al. reported the first cryo-ET/STA high-resolution (9 Å) structure of the glycoprotein B pre-fusion complex illustrating the power of cryo-ET to reveal previously uncharacterized structures that also have importance for immunogen and vaccine design and development [65].

Members of the *Filoviridae* family, such as Ebola, Marburg, and Sudan viruses contain a non-segmented, single-stranded negative-sense RNA genome and can cause hemorrhagic fever and severe disease. The RNPs of Ebola virus are helical scaffolds made up of the viral genome wrapped up in viral nucleoprotein (NP), VP24 and VP35 virus proteins. Ebola virion budding is driven by the matrix protein (VP40) self-assembly and recruitment of RNPs at the inner leaflet of the plasma membrane, resulting in long filamentous virions with branching topology and irregularly shapes [66]. As shown in Figure 1D, STA with helical reconstruction revealed at ∼7 Å resolution that *in vitro* reconstituted Ebola native RNPs are left-handed, most likely contain NP, VP24, VP35, and VP40 and have indistinguishable characteristics from virus particles released from infected cells [67,68]. In this study, STA also revealed high-resolution molecular details about the NP carboxy-terminal extended α-helix important for RNP assembly and recruitment of accessory proteins [67].

Recently there have been several high-resolution cryo-ET/STA studies reporting previously uncharacterized structures of matrix protein layers within purified virions, including HIV-1 [69], IAV [70], RSV [71,72], and Ebola virus [73]. Conley et al. [71] and Sibert et al. [72] used cryo-ET and STA to image RSV released from infected cells that were grown on EM grids. Their results elegantly showed that the helical lattice-like sheet of M protein tightly associated to the inner leaflet of the membrane is reminiscent of the unit cell of the RSV matrix crystal structure and that M likely coordinates the helical ordering of pairs of viral glycoproteins [71,72] (Figure 1E). Similar studies using cryo-ET and STA (∼8 Å) on IAV showed the matrix protein (M1) forms polymers in helical assemblies and provided insights into virus assembly and disassembly (Figure 1F) [70]. To sum up, these studies demonstrate the huge capacity of cryo-ET to improve our understanding of the molecular architecture, mechanism of entry, assembly and dissemination of different viruses at high-resolution and highlights its ability to reveal novel drug targets and for the development of potential therapeutics and vaccines.

Cryo-ET investigation of *in situ* infection processes

Recent advancements in cryo-ET allow us to observe the authentic organization of complexes involved in the battle of infection between the virus and the host cell [74]. In this section, we describe how cryo-ET is aiding studies of enveloped virus behaviour within infected cells and advancing our knowledge towards the ultimate goal of capturing the entire virus life cycle by simply imaging an infected mammalian cell in 3D and at unprecedented resolution. In this approach, mammalian cells are usually seeded on EM grids, and optimal conditions are found under which the cells are able to attach and spread on the grid's support film. This facilitates electron imaging of the peripheral cytoplasmic regions at the thinner, electron-transparent cell edges [75]. However, due to the inelastic mean free path in biological samples, electrons cannot penetrate through cellular regions thicker than 500 nm without multiple scattering and therefore, imaging using this approach is technically challenging. Despite this, extensive areas of peripheral thin-edges can be sufficiently thin for imaging and are perfect for looking at entry and exit mechanisms of envelope viruses at the plasma membrane.

This workflow has been used in human cells to visualize IAVs attached or proximal to the plasma membrane [76], previously unrecognized virus-virus interactions at play during measles virus assembly [77], disassembly of vaccinia virus [78], HIV-1 tethering in restriction, and HIV-1 capsid maturation from viruses released from cells during a typical infection [79,80] and a number of other events during viral infection processes [81].

To successfully assemble and mature, the components of many enveloped virus must traverse through the elaborate network of endomembrane systems of the host cell and access intracellular organelles such as the nucleus. The majority of the host cell endomembrane system such as Golgi apparatus and endoplasmic reticulum has nuclear envelope and ER-Golgi intermediate (ERGIC) compartments. These perinuclear regions are usually too thick for direct cryo-ET imaging and often require auxiliary techniques to thin the sample for subsequent cryo-ET. How these techniques have enabled ground-breaking discoveries in enveloped virus biology are discussed below.

PORTLAND PRESS

Biochemical Society Transactions (2022) **50** 95–105
https://doi.org/10.1042/BST20210433

Assembly of HSV-1 at the nuclear envelope

Cryo-electron microscopy of vitreous sections (CEMOVIS) provides one solution to accessing these important and otherwise inaccessible perinuclear regions. In CEMOVIS, samples are high-pressure frozen and ultrathin cryo-sections of cells and tissues are produced for cryo-ET. This technique has revealed important aspects of HSV-1 virus maturation and assembly at the nuclear envelope. In a landmark study, Hagen et al. [82] used this approach to

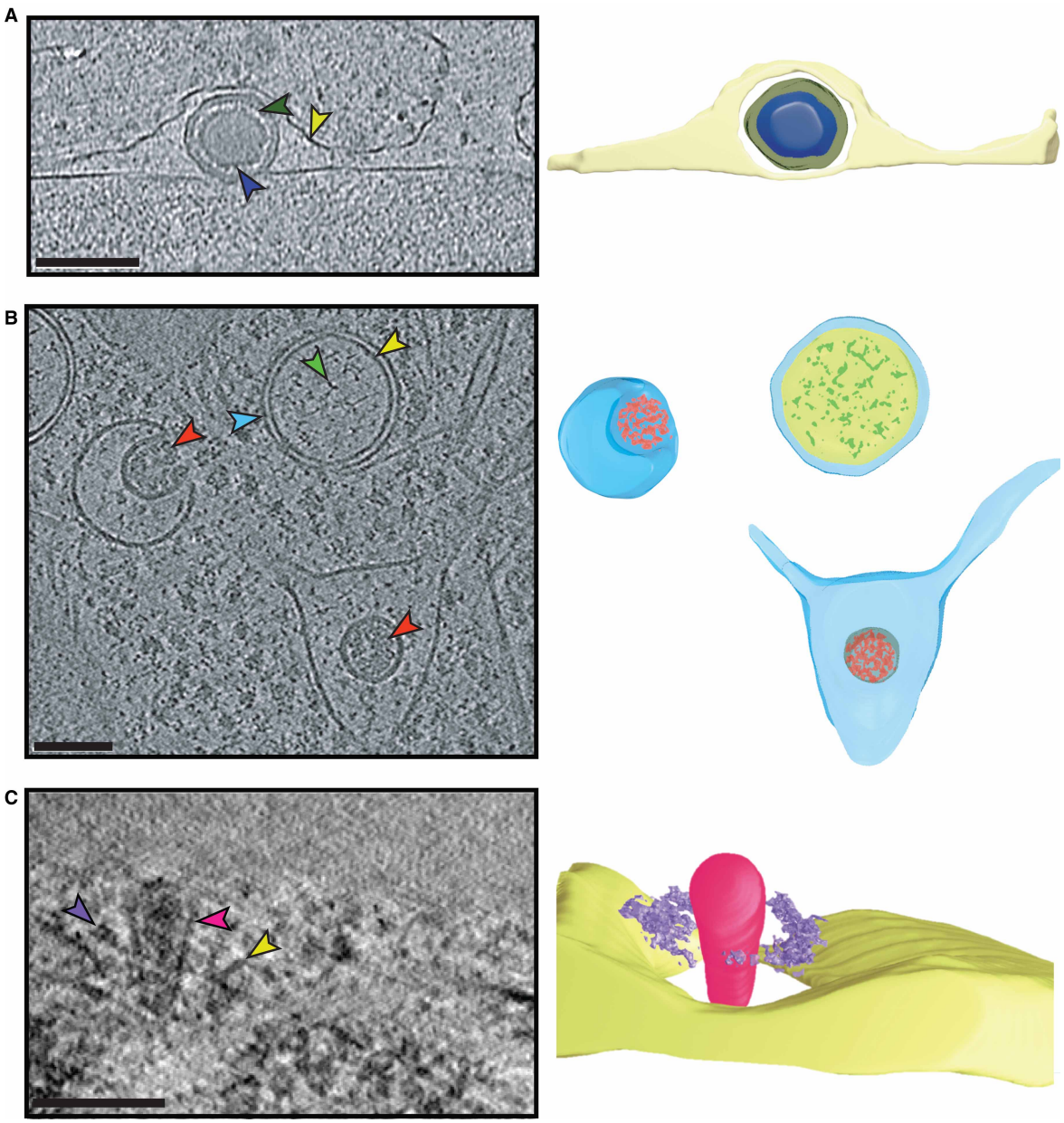

Figure 2. *In situ* cryo-ET of envelope viruses showing aspects of replication.

(**A**) HSV-1 maturation through the nuclear envelope. Blue arrow highlights HSV-1 capsid, dark green arrow highlights the nuclear egress complex, yellow arrow highlights the nuclear envelope membrane. (**B**) SARS-CoV-2 replication. Green arrow highlights viral RNA inside double-membraned viral replication vesicles (cross-section), yellow arrow highlights inner membrane, blue arrow highlights outer membrane of vesicle, red arrows highlight viral RNPs budding into ERGIC. (**C**) Intact HIV-1 capsid cores at the nuclear envelope. Pink arrow indicates an HIV-1 capsid core docked inside a nuclear pore complex (NPC), yellow arrow highlights membrane, and purple arrow highlights cytoplasmic ring of NPC (**A**–**C**) Left panel showing representative tomographic slices and right panel showing corresponding segmented volumes generated using Amira and rendered in Cinama4D. Scale bar 100 nm.

capture the molecular architecture of the HSV-1 virus nuclear egress complex (NEC) (Figure 2A) and gained insights into the mechanism for budding and scission of vesicles at the inner nuclear membrane. In pseudorabies virus (alphaherpesvirus) infected cells, the authors used complementary approaches to reveal these vesicles contained a curved hexagonal lattice composed of two closely opposing layers and proposed the membrane anchored viral pUL34 protein layer was responsible for producing the required curvature needed for their size to closely match herpes virus capsids [82]

Moreover, cryo-sectioning of samples prepared using the Tokuyasu method, a complementary technique to CEMOVIS, has revealed insights concerning HSV-1 maturation by addition of inner tegument protein pUL36 in the nucleus [83]. The CEMOVIS method suffers from sample preparation artefacts (compression, knife-marks and crevasses) and samples are chemically fixed in the Tokuyasu method. Therefore, both methods are not ideal for studying structural details at high-resolution.

Replication of SARS-CoV in ER-derived vesicles

To avoid potential artefacts introduced by CEMOVIS or the Tokuyasu method, cryo-FIB milling can be used to prepare thin lamella of frozen-hydrated cells [84]. Here, plunge frozen mammalian cells grown on EM grids and are placed in a scanning electron microscope (SEM) that is equipped with an ion beam source in addition to the more usual electron gun. Typically, a stream of gallium ions is targeted to the frozen cell, etching regions of the cell to leave a thin electron-transparent lamella. Cryo-FIB milling together with cryo-ET was recently used to access the interior of murine hepatitis coronavirus (MHV) and severe acute respiratory syndrome coronavirus (SARS-CoV) infected cells, and image double-membrane viral replication vesicles in the cytoplasm in 3D [55,85] (Figure 2B). This revealed a long-standing question in the field of how the viral RNA inside double-membrane vesicles can gain access to the cytosol for RNP entrapment, RNP budding and egress into the ERGIC (Figure 2B). Wolf et al. used cryo-FIB milling in combination with cryo-ET to determine the precise structural details of these vesicles. Importantly, they discovered a large pore embedded in the double-membrane of MHV infected cells. STA showed that this pore exhibited hexameric architecture, likely containing the large viral transmembrane protein nsp3 (nonstructural protein 3). To illustrate this, the authors, performed an elegant infection experiment whereby they tagged nsp3 with eGFP, and subsequent STA revealed the presence of six additional densities on top of the cytosolic crown-like hexameric structure [85].

Intact HIV-1 capsids at the nuclear envelope

In a recent ground-breaking study, Zila et al. infected clinically relevant human CD4+ T cells with HIV-1 virus displaying native HIV-1 spike protein. Imaging of these infected cells with cryo-FIB milling and cryo-ET captured intact HIV-1 capsid cores at the nuclear envelope [12] (Figure 2C). STA confirmed the presence of individual hexameric capsid proteins within these HIV-1 cores and also revealed they fracture once they enter the nucleus. This observation strengthened the model which proposed uncoating occurs at nuclear pores, as opposed to uncoating upon entry or cytoplasmic uncoating.

Conclusion

Understanding architectures of different viruses and the structural basis of their infection, replication and dissemination are key to understanding the fundamental biological properties of viruses. Recent advances in microscopes, detectors and data processing software have enabled cryo-ET to deliver structures of macromolecular complexes at near-atomic resolution. In this review, we have highlighted a few examples where cryo-ET, together with cryo-FIB milling, have provided key insights into the structure and infection processes of several enveloped viruses. It is imperative that in the coming years, cryo-ET will become an indispensable tool to study structural details of viruses and reveal the complex molecular interplay between viruses and their hosts at unprecedented resolution.

Perspectives

- Cryo-ET is unique in its ability to reveal structures of pleomorphic enveloped viruses in their native cellular environment and shed light on their mechanisms of entry, replication, assembly, maturation and egress during infection at unprecedented resolution.

Biochemical Society Transactions (2022) **50** 95–105
https://doi.org/10.1042/BST20210433

- While X-ray crystallography, nuclear magnetic resonance (NMR) spectroscopy and cryo-EM SPA are now routinely used to yield atomic structures of protein complexes, these methods are limited to specimens that can be purified and remain stable in solution. Super-resolution microscopy can be used to study large protein complexes *in situ* but only at ∼50 nm resolution. Cryo-ET together with STA uniquely bridges this resolution gap and enables the study of protein complexes *in situ* at 2–4 nm (or in favourable cases, at sub-nanometer) resolution.

- Although advances in cryo-ET and associated techniques have enabled visualization of architectures and life cycles of many critical viruses, steps involving data collection and processing are still challenging and have low throughput. Technical developments in these fronts will make cryo-ET an even more attractive tool to structural virologists and augment its contribution to drug/vaccine development.

Competing Interests

The authors declare that there are no competing interests associated with the manuscript.

Acknowledgements

We apologize to all our colleagues whose significant contributions could not be cited due to space limitations. The authors thank Martin Beck, Kay Grunewald and Montserrat Bárcena for generously sharing materials used in Figure 2. We thank David Bhella, Pablo Murcia, Michaela Conley, and Meredith Stewart for their critical reading of the manuscript.

Funding

DG is supported by an NHMRC grant (APP1196924). S.C. is supported by Medical Research Council grant (MC_UU_12014/7). D.C.S. supported by the Melbourne Research Scholarship.

Author Contributions

D.G., S.D.C., and N.V. conceived the manuscript; N.V., S.D.C., D.G. wrote the manuscript; S.D.C., D.C.S., D.G. designed figures. All authors edited the manuscript.

Abbreviations

AIDS, acquired immunodeficiency syndrome; CA, capsid protein; CEMOVIS, Cryo-electron microscopy of vitreous sections; CLEM, correlative light and electron microscopy; COVID-19, coronavirus disease; CTD, C-terminal domain; ERGIC, ER-Golgi intermediate; HSV-1, Herpes simplex virus 1; IAV, influenza A virus; MHV, murine hepatitis coronavirus; NC, nucleocapsid; NP, nucleoprotein; NTD, N-terminal domain; RNP, ribonucleoprotein; RSV, respiratory syncytial virus; SPA, single particle analysis; STA, subtomogram averaging.

References

1 Welsch, S., Müller, B. and Kräusslich, H.-G. (2007) More than one door: budding of enveloped viruses through cellular membranes. *FEBS Lett.* **581**, 2089–2097 https://doi.org/10.1016/j.febslet.2007.03.060
2 Rheinemann, L. and Sundquist, W.I. (2021) Virus budding. *Encyclopedia Virol.*, 519–528 https://doi.org/10.1016/B978-0-12-814515-9.00023-0
3 Gristick, H.B., von Boehmer L, West A.P., Schamber, M., Gazumyan, A., Golijanin, J. et al. (2016) Natively glycosylated HIV-1 Env structure reveals new mode for antibody recognition of the CD4-binding site. *Nat. Struct. Mol. Biol.* **23**, 906–915 https://doi.org/10.1038/nsmb.3291
4 Watanabe, Y., Bowden, T.A., Wilson, I.A. and Crispin, M. (2019) Exploitation of glycosylation in enveloped virus pathobiology. *Biochim. Biophys. Acta Gen. Subj.* **1863**, 1480–1497 https://doi.org/10.1016/j.bbagen.2019.05.012
5 Dimitrov, D.S. (2004) Virus entry: molecular mechanisms and biomedical applications. *Nat. Rev. Microbiol.* **2**, 109–122 https://doi.org/10.1038/nrmicro817
6 Wolff, G., Melia, C.E., Snijder, E.J. and Bárcena, M. (2020) Double-membrane vesicles as platforms for viral replication. *Trends Microbiol.* **28**, 1022–1033 https://doi.org/10.1016/j.tim.2020.05.009
7 Ghosal, D., Kaplan, M., Chang, Y.-W. and Jensen, G.J. (2019) *In situ* imaging and structure determination of bacterial toxin delivery systems using electron cryotomography. *Methods Mol. Biol.* **1921**, 249–265 https://doi.org/10.1007/978-1-4939-9048-1_16
8 Tegunov, D., Xue, L., Dienemann, C., Cramer, P. and Mahamid, J. (2021) Multi-particle cryo-EM refinement with M visualizes ribosome-antibiotic complex at 3.5 Å in cells. *Nat. Methods* **18**, 186–193 https://doi.org/10.1038/s41592-020-01054-7

9 Carter, S.D., Hampton, C.M., Langlois, R., Melero, R., Farino, Z.J., Calderon, M.J. et al. (2020) Ribosome-associated vesicles: a dynamic subcompartment of the endoplasmic reticulum in secretory cells. *Sci. Adv.* **6**, eaay9572 https://doi.org/10.1126/sciadv.aay9572
10 Ghosal, D., Kim, K.W., Zheng, H., Kaplan M., Truchan H.K., Lopez A.E. et al. (2019) *In vivo* structure of the Legionella type II secretion system by electron cryotomography. *Nat. Microbiol/* **4**, 2101–2108 https://doi.org/10.1038/s41564-019-0603-6
11 Ghosal, D., Jeong, K.C., Chang, Y.-W., Gyore, J., Teng, L., Gardner, A. et al. (2019) Molecular architecture, polar targeting and biogenesis of the Legionella Dot/Icm T4SS. *Nat. Microbiol.* **4**, 1173–1182 https://doi.org/10.1038/s41564-019-0427-4
12 Zila, V., Margiotta, E., Turoňová, B., Müller, T.G., Zimmerli, C.E., Mattei, S. et al. (2021) Cone-shaped HIV-1 capsids are transported through intact nuclear pores. *Cell* **184**, 1032–1046.e18 https://doi.org/10.1016/j.cell.2021.01.025
13 Hu, B., Morado, D.R., Margolin, W., Rohde, J.R., Arizmendi, O., Picking, W.L. et al. (2015) Visualization of the type III secretion sorting platform of *Shigella flexneri*. *Proc. Natl Acad. Sci. U.S.A.* **112**, 1047–1052 https://doi.org/10.1073/pnas.1411610112
14 Bammes, B.E., Rochat, R.H., Jakana, J., Chen, D.-H. and Chiu, W. (2012) Direct electron detection yields cryo-EM reconstructions at resolutions beyond 3/4 Nyquist frequency. *J. Struct. Biol.* **177**, 589–601 https://doi.org/10.1016/j.jsb.2012.01.008
15 Danev, R., Buijsse, B., Khoshouei, M., Plitzko, J.M. and Baumeister, W. (2014) Volta potential phase plate for in-focus phase contrast transmission electron microscopy. *Proc. Natl Acad. Sci. U.S.A.* **111**, 15635–15640 https://doi.org/10.1073/pnas.1418377111
16 Guo, Q., Lehmer, C., Martínez-Sánchez, A., Rudack, T., Beck, F., Hartmann, H. et al. (2018) In situ structure of neuronal C9orf72 poly-GA aggregates reveals proteasome recruitment. *Cell* **172**, 696–705.e12 https://doi.org/10.1016/j.cell.2017.12.030
17 Zachs, T., Schertel, A., Medeiros, J., Weiss, G.L., Hugener J., Matos, J. et al. (2020) Fully automated, sequential focused ion beam milling for cryo-electron tomography. *eLife* **9**, e52286 https://doi.org/10.7554/eLife.52286
18 Deeks, S.G., Overbaugh, J., Phillips, A. and Buchbinder, S. (2015) HIV infection. *Nat. Rev. Dis. Primers* **1**, 1–22 https://doi.org/10.1038/nrdp.2015.35
19 Cunningham, A.L., Donaghy, H., Harman, A.N., Kim, M. and Turville, S.G. (2010) Manipulation of dendritic cell function by viruses. *Curr. Opin. Microbiol.* **13**, 524–529 https://doi.org/10.1016/j.mib.2010.06.002
20 World Health Organization. (2021) *Global Progress Report on HIV, Viral Hepatitis and Sexually Transmitted Infections, 2021: Accountability for the Global Health Sector Strategies 2016–2021: Actions for Impact*, World Health Organization
21 Campbell, E.M. and Hope, T.J. (2015) HIV-1 capsid: the multifaceted key player in HIV-1 infection. *Nat. Rev. Microbiol.* **13**, 471–483 https://doi.org/10.1038/nrmicro3503
22 Hulme, A.E., Perez, O. and Hope, T.J. (2011) Complementary assays reveal a relationship between HIV-1 uncoating and reverse transcription. *Proc. Natl Acad. Sci. U.S.A.* **108**, 9975–9980 https://doi.org/10.1073/pnas.1014522108
23 Sundquist, W.I. and Kräusslich, H.-G. (2012) HIV-1 assembly, budding, and maturation. *Cold Spring Harb. Perspect. Med.* **2**, a006924 https://doi.org/10.1101/cshperspect.a006924
24 Bejarano, D.A., Puertas, M.C., Börner, K., Martinez-Picado, J., Müller, B. and Kräusslich, H.-G. (2018) Detailed characterization of early HIV-1 replication dynamics in primary human macrophages. *Viruses* **10**, E620 https://doi.org/10.3390/v10110620
25 Bejarano, D.A., Peng, K., Laketa, V., Börner, K., Jost, K.L., Lucic, B. et al. (2019) HIV-1 nuclear import in macrophages is regulated by CPSF6-capsid interactions at the nuclear pore complex. *eLife* **8**, e41800 https://doi.org/10.7554/eLife.41800
26 Chen, N.-Y., Zhou, L., Gane, P.J., Opp, S., Ball, N.J., Nicastro, G. et al. (2016) HIV-1 capsid is involved in post-nuclear entry steps. *Retrovirology* **13**, 28 https://doi.org/10.1186/s12977-016-0262-0
27 Chin, C.R., Perreira, J.M., Savidis, G., Portmann, J.M., Aker, A.M., Feeley, E.M. et al. (2015) Direct visualization of HIV-1 replication intermediates shows that viral capsid and CPSF6 modulate HIV-1 intra-nuclear invasion and integration. *Cell Rep.* **13**, 1717–1731 https://doi.org/10.1016/j.celrep.2015.10.036
28 Hulme, A.E., Kelley, Z., Foley, D. and Hope, T.J. (2015) Complementary assays reveal a low level of CA associated with viral complexes in the nuclei of HIV-1-infected cells. *J. Virol.* **89**, 5350–5361 https://doi.org/10.1128/JVI.00476-15
29 Peng, K., Muranyi, W., Glass, B., Laketa, V., Yant, S.R., Tsai, L. et al. (2014) Quantitative microscopy of functional HIV post-entry complexes reveals association of replication with the viral capsid. *eLife* **3**, e04114 https://doi.org/10.7554/eLife.04114
30 Siliciano, R.F. and Greene, W.C. (2011) HIV latency. *Cold Spring Harb. Perspect. Med.* **1**, a007096 https://doi.org/10.1101/cshperspect.a007096
31 Briggs, J.A.G., Riches, J.D., Glass, B., Bartonova, V., Zanetti, G. and Kräusslich, H.-G. (2009) Structure and assembly of immature HIV. *Proc. Natl Acad. Sci. U.S.A.* **106**, 11090–11095 https://doi.org/10.1073/pnas.0903535106
32 Inamdar, K., Tsai, F.-C., Dibsy, R., de Poret, A., Manzi, J., Merida, P. et al. (2021) Full assembly of HIV-1 particles requires assistance of the membrane curvature factor IRSp53. *eLife* **10**, e67321 https://doi.org/10.7554/eLife.67321
33 Johnson, D.S., Bleck, M. and Simon, S.M. (2018) Timing of ESCRT-III protein recruitment and membrane scission during HIV-1 assembly. *eLife* **7**, e36221 https://doi.org/10.7554/eLife.36221
34 Zhao, G., Perilla, J.R., Yufenyuy, E.L., Meng, X., Chen, B., Ning, J. et al. (2013) Mature HIV-1 capsid structure by cryo-electron microscopy and all-atom molecular dynamics. *Nature* **497**, 643–646 https://doi.org/10.1038/nature12162
35 Mattei, S., Glass, B., Hagen, W.J.H., Kräusslich, H.-G. and Briggs, J.A.G. (2016) The structure and flexibility of conical HIV-1 capsids determined within intact virions. *Science* **354**, 1434–1437 https://doi.org/10.1126/science.aah4972
36 Turoňová, B., Hagen, W.J.H., Obr, M., Mosalaganti, S., Beugelink, J.W., Zimmerli, C.E. et al. (2020) Benchmarking tomographic acquisition schemes for high-resolution structural biology. *Nat. Commun.* **11**, 876 https://doi.org/10.1038/s41467-020-14535-2
37 Turoňová, B., Schur, F.K.M., Wan, W. and Briggs, J.A.G. (2017) Efficient 3D-CTF correction for cryo-electron tomography using NovaCTF improves subtomogram averaging resolution to 3.4 Å. *J. Struct. Biol.* **199**, 187–195 https://doi.org/10.1016/j.jsb.2017.07.007
38 de Marco, A., Müller, B., Glass, B., Riches, J.D., Kräusslich, H.-G., Briggs, J.A.G. et al. (2010) Structural analysis of HIV-1 maturation using cryo-electron tomography. *PLoS Pathog.* **6**, e1001215 https://doi.org/10.1371/journal.ppat.1001215
39 Schur, F.K.M., Hagen, W.J.H., Rumlová, M., Ruml, T., Müller, B., Kräusslich, H.-G. et al. (2015) Structure of the immature HIV-1 capsid in intact virus particles at 8.8 Å resolution. *Nature* **517**, 505–508 https://doi.org/10.1038/nature13838
40 Mendonça, L., Sun, D., Ning, J., Liu, J., Kotecha, A., Olek, M. et al. (2021) CryoET structures of immature HIV Gag reveal six-helix bundle. *Commun. Biol.* **4**, 481 https://doi.org/10.1038/s42003-021-01999-1
41 Schur, F.K.M., Obr, M., Hagen, W.J.H., Wan, W., Jakobi, A.J., Kirkpatrick, J.M. et al. (2016) An atomic model of HIV-1 capsid-SP1 reveals structures regulating assembly and maturation. *Science* **353**, 506–508 https://doi.org/10.1126/science.aaf9620

42 Tan, A., Pak, A.J., Morado, D.R., Voth, G.A. and Briggs, J.A.G. (2021) Immature HIV-1 assembles from Gag dimers leaving partial hexamers at lattice edges as potential substrates for proteolytic maturation. *Proc. Natl Acad. Sci. U.S.A.* **118**, e2020054118 https://doi.org/10.1073/pnas.2020054118
43 Gibson, P.G., Qin, L. and Puah, S.H. (2020) COVID-19 acute respiratory distress syndrome (ARDS): clinical features and differences from typical pre-COVID-19 ARDS. *Med. J. Aust.* **213**, 54–56.e1 https://doi.org/10.5694/mja2.50674
44 Hoffmann, M., Kleine-Weber, H., Schroeder, S., Krüger, N., Herrler, T., Erichsen, S. et al. (2020) SARS-CoV-2 cell entry depends on ACE2 and TMPRSS2 and is blocked by a clinically proven protease inhibitor. *Cell* **181**, 271–280.e8 https://doi.org/10.1016/j.cell.2020.02.052
45 Petersen, E., Koopmans, M., Go, U., Hamer, D.H., Petrosillo, N., Castelli, F. et al. (2020) Comparing SARS-CoV-2 with SARS-CoV and influenza pandemics. *Lancet Infect. Dis.* **20**, e238–e244 https://doi.org/10.1016/S1473-3099(20)30484-9
46 Vankadari, N. and Wilce, J.A. (2020) Emerging wuHan (COVID-19) coronavirus: glycan shield and structure prediction of spike glycoprotein and its interaction with human CD26. *Emerg. Microbes Infect.* **9**, 601–604 https://doi.org/10.1080/22221751.2020.1739565
47 Wrapp, D., Wang, N., Corbett, K.S., Goldsmith, J.A., Hsieh, C.-L., Abiona, O. et al. (2020) Cryo-EM structure of the 2019-nCoV spike in the prefusion conformation. *Science* **367**, 1260–1263 https://doi.org/10.1126/science.abb2507
48 Barnes, C.O., West, A.P., Huey-Tubman, K.E., Hoffmann, M.A.G., Sharaf, N.G., Hoffman, P.R. et al. (2020) Structures of human antibodies bound to SARS-CoV-2 spike reveal common epitopes and recurrent features of antibodies. *Cell* **182**, 828–842.e16 https://doi.org/10.1016/j.cell.2020.06.025
49 Bangaru, S., Ozorowski, G., Turner, H.L., Antanasijevic, A., Huang, D., Wang, X. et al. (2020) Structural analysis of full-length SARS-CoV-2 spike protein from an advanced vaccine candidate. *Science* **370**, 1089–1094 https://doi.org/10.1126/science.abe1502
50 Du Toit, A. (2020) Coronavirus replication factories. *Nat. Rev. Microbiol.* **18**, 411–411 https://doi.org/10.1038/s41579-020-0406-z
51 Ke, Z., Oton, J., Qu, K., Cortese, M., Zila, V., McKeane, L. et al. (2020) Structures and distributions of SARS-CoV-2 spike proteins on intact virions. *Nature* **588**, 498–502 https://doi.org/10.1038/s41586-020-2665-2
52 Liu, C., Mendonça, L., Yang, Y., Gao, Y., Shen, C., Liu, J. et al. (2020) The architecture of inactivated SARS-CoV-2 with postfusion spikes revealed by cryo-EM and cryo-ET. *Structure* **28**, 1218–1224.e4 https://doi.org/10.1016/j.str.2020.10.001
53 Turoňová, B., Sikora, M., Schürmann, C., Hagen, W.J.H., Welsch, S., Blanc, F.E.C. et al. (2020) In situ structural analysis of SARS-CoV-2 spike reveals flexibility mediated by three hinges. *Science* **370**, 203–208 https://doi.org/10.1126/science.abd5223
54 Yao, H., Song, Y., Chen, Y., Wu, N., Xu, J., Sun, C. et al. (2020) Molecular architecture of the SARS-CoV-2 virus. *Cell* **183**, 730–738.e13 https://doi.org/10.1016/j.cell.2020.09.018
55 Klein, S., Cortese, M., Winter, S.L., Wachsmuth-Melm, M., Neufeldt, C.J., Cerikan, B. et al. (2020) SARS-CoV-2 structure and replication characterized by in situ cryo-electron tomography. *Nat. Commun.* **11**, 5885 https://doi.org/10.1038/s41467-020-19619-7
56 Rey, F.A. and Lok, S.-M. (2018) Common features of enveloped viruses and implications for immunogen design for next-Generation vaccines. *Cell* **172**, 1319–1334 https://doi.org/10.1016/j.cell.2018.02.054
57 Booy, F.P., Newcomb, W.W., Trus, B.L., Brown, J.C., Baker, T.S. and Steven, A.C. (1991) Liquid-crystalline, phage-like packing of encapsidated DNA in herpes simplex virus. *Cell* **64**, 1007–1015 https://doi.org/10.1016/0092-8674(91)90324-R
58 Buch, M.H.C., Newcomb, W.W., Winkler, D.C., Steven, A.C. and Heymann, J.B. (2021) Cryo-electron tomography of the herpesvirus procapsid reveals interactions of the portal with the scaffold and a shift on maturation. *mBio* **12**, e03575-20 https://doi.org/10.1128/mBio.03575-20
59 Cardone, G., Winkler, D.C., Trus, B.L., Cheng, N., Heuser, J.E., Newcomb, W.W. et al. (2007) Visualization of the herpes simplex virus portal in situ by cryo-electron tomography. *Virology* **361**, 426–434 https://doi.org/10.1016/j.virol.2006.10.047
60 Chang, J.T., Schmid, M.F., Rixon, F.J. and Chiu, W. (2007) Electron cryotomography reveals the portal in the herpesvirus capsid. *J. Virol.* **81**, 2065–2068 https://doi.org/10.1128/JVI.02053-06
61 Schmid, M.F., Hecksel, C.W., Rochat, R.H., Bhella, D., Chiu, W. and Rixon, F.J. (2012) A tail-like assembly at the portal vertex in intact herpes simplex type-1 virions. *PLoS Pathog.* **8**, e1002961 https://doi.org/10.1371/journal.ppat.1002961
62 Grünewald, K., Desai, P., Winkler, D.C., Heymann, J.B., Belnap, D.M., Baumeister, W. et al. (2003) Three-Dimensional structure of herpes simplex virus from cryo-electron tomography. *Science* **302**, 1396–1398 https://doi.org/10.1126/science.1090284
63 Newcomb, W.W., Fontana, J., Winkler, D.C., Cheng, N., Heymann, J.B. and Steven, A.C. (2017) The primary enveloped virion of herpes simplex virus 1: its role in nuclear egress. *mBio* **8**, e00825-17 https://doi.org/10.1128/mBio.00825-17
64 Zeev-Ben-Mordehai, T., Vasishtan, D., Durán, A.H., Vollmer, B., White, P., Pandurangan, A.P. et al. (2016) Two distinct trimeric conformations of natively membrane-anchored full-length herpes simplex virus 1 glycoprotein B. *Proc. Natl Acad. Sci. U.S.A.* **113**, 4176–4181 https://doi.org/10.1073/pnas.1523234113
65 Vollmer, B., Pražák, V., Vasishtan, D., Jefferys, E.E., Hernandez-Duran, A., Vallbracht, M. et al. (2020) The prefusion structure of herpes simplex virus glycoprotein B. *Sci. Adv.* **6**, eabc1726 https://doi.org/10.1126/sciadv.abc1726
66 Bornholdt, Z.A., Noda, T., Abelson, D.M., Halfmann, P., Wood, M., Kawaoka, Y. et al. (2013) Structural basis for ebolavirus matrix assembly and budding; protein plasticity allows multiple functions. *Cell* **154**, 763–774 https://doi.org/10.1016/j.cell.2013.07.015
67 Wan, W., Kolesnikova, L., Clarke, M., Koehler, A., Noda, T., Becker, S. et al. (2017) Structure and assembly of the Ebola virus nucleocapsid. *Nature* **551**, 394–397 https://doi.org/10.1038/nature24490
68 Bharat, T.A.M., Noda, T., Riches, J.D., Kraehling, V., Kolesnikova, L., Becker, S. et al. (2012) Structural dissection of Ebola virus and its assembly determinants using cryo-electron tomography. *Proc. Natl Acad. Sci. U.S.A.* **109**, 4275–4280 https://doi.org/10.1073/pnas.1120453109
69 Qu, K., Ke, Z., Zila, V., Anders-Össwein, M., Glass, B., Mücksch, F. et al. (2021) Maturation of the matrix and viral membrane of HIV-1. *Science* **373**, 700–704 https://doi.org/10.1126/science.abe6821
70 Peukes, J., Xiong, X., Erlendsson, S., Qu, K., Wan, W., Calder, L.J. et al. (2020) The native structure of assembled influenza A virus M1 matrix protein. *Nature* **587**, 495–498 https://doi.org/10.1038/s41586-020-2696-8
71 Conley, M.J., Short, J.M., Burns, A.M., Streetley, J., Hutchings, J., Bakker, S.E. et al. (2021) Helical ordering of envelope associated proteins and glycoproteins in respiratory syncytial virus filamentous virions. *bioRxiv* https://doi.org/10.1101/2021.08.04.455049
72 Sibert, B.S., Kim, J.Y., Yang, J.E., Ke, Z., Stobart, C.C., Moore, M.M. et al. (2021) Respiratory syncytial virus matrix protein assembles as a lattice with local and extended order that coordinates the position of the fusion glycoprotein. *bioRxiv* https://doi.org/10.1101/2021.10.13.464285
73 Wan, W., Clarke, M., Norris, M.J., Kolesnikova, L., Koehler, A., Bornholdt, Z.A. et al. (2020) Ebola and Marburg virus matrix layers are locally ordered assemblies of VP40 dimers. *eLife* **9**, e59225 https://doi.org/10.7554/eLife.59225

74 Carter, S.D., Mamede, J.I., Hope, T.J. and Jensen, G.J. (2020) Correlated cryogenic fluorescence microscopy and electron cryo-tomography shows that exogenous TRIM5α can form hexagonal lattices or autophagy aggregates in vivo. *Proc. Natl Acad. Sci. U.S.A.* **117**, 29702–29711 https://doi.org/10.1073/pnas.1920323117
75 Medalia, O., Weber, I., Frangakis, A.S., Nicastro, D., Gerisch, G. and Baumeister, W. (2002) Macromolecular architecture in eukaryotic cells visualized by cryoelectron tomography. *Science* **298**, 1209–1213 https://doi.org/10.1126/science.1076184
76 Vijayakrishnan, S., Loney, C., Jackson, D., Suphamungmee, W., Rixon, F.J. and Bhella, D. (2013) Cryotomography of budding influenza A virus reveals filaments with diverse morphologies that mostly do not bear a genome at their distal end. *PLoS Pathog.* **9**, e1003413 https://doi.org/10.1371/journal.ppat.1003413
77 Ke, Z., Strauss, J.D., Hampton, C.M., Brindley, M.A., Dillard, R.S., Leon, F. et al. (2018) Promotion of virus assembly and organization by the measles virus matrix protein. *Nat. Commun.* **9**, 1736 https://doi.org/10.1038/s41467-018-04058-2
78 Cyrklaff, M., Linaroudis, A., Boicu, M., Chlanda, P., Baumeister, W., Griffiths, G. et al. (2007) Whole cell cryo-electron tomography reveals distinct disassembly intermediates of vaccinia virus. *PLoS ONE* **2**, e420 https://doi.org/10.1371/journal.pone.0000420
79 Carlson, L.-A., de Marco, A., Oberwinkler, H., Habermann, A., Briggs, J.A.G., Kräusslich, H.G. et al. (2010) Cryo electron tomography of native HIV-1 budding sites. *PLoS Pathog.* **6**, e1001173 https://doi.org/10.1371/journal.ppat.1001173
80 Woodward, C.L., Cheng, S.N. and Jensen, G.J. (2015) Electron cryotomography studies of maturing HIV-1 particles reveal the assembly pathway of the viral core. *J. Virol.* **89**, 1267–1277 https://doi.org/10.1128/JVI.02997-14
81 Chmielewski, D., Schmid, M.F., Simmons, G., Jin, J. and Chiu, W. (2021) *In situ* alphavirus assembly and budding mechanism revealed by cellular cryoET. *bioRxiv* https://doi.org/10.1101/2021.10.14.464449
82 Hagen, C., Dent, K.C., Zeev-Ben-Mordehai, T., Grange, M., Bosse, J.B., Whittle, C. et al. (2015) Structural basis of vesicle formation at the inner nuclear membrane. *Cell* **163**, 1692–1701 https://doi.org/10.1016/j.cell.2015.11.029
83 Vijayakrishnan, S., McElwee, M., Loney, C., Rixon, F. and Bhella, D. (2020) *In situ* structure of virus capsids within cell nuclei by correlative light and cryo-electron tomography. *Sci. Rep.* **10**, 17596 https://doi.org/10.1038/s41598-020-74104-x
84 Mahamid, J., Pfeffer, S., Schaffer, M., Villa, E., Danev, R., Cuellar, L.K. et al. (2016) Visualizing the molecular sociology at the HeLa cell nuclear periphery. *Science* **351**, 969–972 https://doi.org/10.1126/science.aad8857
85 Wolff, G., Limpens, R.W.A.L., Zevenhoven-Dobbe, J.C., Laugks, U., Zheng, S., de Jong, A.W.M. et al. (2020) A molecular pore spans the double membrane of the coronavirus replication organelle. *Science* **369**, 1395–1398 https://doi.org/10.1126/science.abd3629